Application of TRMM/PR Data for Numerical Simulations with Mesoscale Model MM5

XU Zhifang*[1] (徐枝芳), GE Wenzhong[1] (葛文忠), DANG Renqing[1] (党人庆),
Toshio IGUCHI[2], and Takao TAKADA[3]

[1] *Department of Atmospheric Sciences, Nanjing University, Nanjing* 210093

[2] *Communications Research Laboratory, Nukui Kitamachi* 4-2-1, *Koganei, Tokyo* 184, *Japan*

[3] *Institute for Hydrospheric Atmospheric Sciences, Nagoya University, Japan*

(Received April 18, 2002; revised October 18, 2002)

ABSTRACT

Numerical simulations of two heavy rainfall cases in the Changjiang-Huaihe River basin are performed with TRMM/PR (precipitation radar) data incorporated into the PSU/NCAR meso scale model MM5. The mixing ratio of rainwater q_r is obtained from the $R-q_r$ relation (R is the rainfall rate), and the mixing ratio of water vapor q_v in the model is replaced by $q'_v = q_v + q_r$. Then, TRMM/PR data are used to modify humidity analysis obtained from conventional radiosonde data, and sensitivity experiments (STE) are performed and compared to control experiments (CTL). Results show that both the heavy rainfall distribution and its maximum amounts from STE are improved compared with those from CTL.

Key words: TRMM /PR, numerical simulation, mixing ratio of rainwater, mixing ratio of vapor, heavy rainfall, spin-up problem, cumulus parameterization scheme

1. Introduction

During the last two decades, mesoscale models have been used to study rainstorms, and continuous progress has been made. But some problems still exist when using mesoscale models to do real-time prediction or simulation. One of the problems is due to data, since the initial field for numerical simulations or predictions ordinarily uses radiosonde data, which mainly contains large-scale weather systems since the average distance between radiosonde stations is about 300 km, but meso scale and microscale systems which are directly related to rainstorms are often missed. This deficiency leads to deviations of distribution and maximum values of simulated or predicted rainfall. However, incorporating satellite or radar data with higher temporal and spatial resolutions into the mesoscale model can improve this deficiency. As noted by Turpeinen et al. (1990), numerical weather prediction models are still plagued in forecasting appropriate amounts of precipitation during the first 12 hours of integration. This is the so called spin-up problem of condensation and precipitation. Since the 1980s, this problem has been worked on in order to shorten the spin-up time and increase the predicted rainfall amount. Researchers have made use of radar or satellite data in the model for resolving these problems. Examples are as follows: (1) Wolcott and Warner (1981) and Jiang et al. (1994) applied satellite data and rainfall observation at the initial time for modifying the initial humidity field in the numerical simulation. (2) Ninomiya and Kurihara (1987) made use of IR satellite data for the forecast experiment of a long-lived mesoscale convective system in the Baiu frontal zone. (3) Turpeinen et al. (1990) incorporated the latent heat forcing by using IR and VIS satellite data into the Canadian regional finite-element model with static initialization. (4) Wang and Warner (1988) estimated the radar-based precipitation rate and used hourly rain gauge data to define a three-dimensional latent heating rate field that contributes to the diabatic heating term in the model's thermodynamic equation during the forecast period. (5) Mills and Davidson (1987) proposed a system for deriving tropospheric moisture profiles from GMS IR satellite imagery. (6) Guo et al. (1999) studied the use of radar data in the numerical

*E-mail: xusister@yahoo.com.cn

simulation of heavy rainfall in the Changjiang-Huaihe River Basin. (7) Ge et al. (1998, 1999, 2000) applied both radar and satellite data for the real-time numerical experiment and simulation of heavy rainfall and obtained better results. In the above-mentioned work, some researchers pointed out that it was important that the humidity around the rainfall region was improved when radar and satellite data were incorporated into meso scale models. Further more, Walcott and Warner (1981) emphasized the importance of the adjustment of the humidity accompanying the diabatic initialization, and argued that if the environment is not humid enough, the upward motion associated with the initialized divergence field will not be sustained by latent heat release. In 1997, Sun and Crook assimilated radar data into a cloud model with the $Z - q_r$ relationship (Z is the radar reflectivity factor). They found that assimilating the rainwater mixing ratio q_r obtained from the reflectivity data Z, results in a better performance of the retrieval procedure than directly assimilating the reflectivity, and that the technique is robust to calibration errors in reflectivity. In this paper, we consider Sun and Crook's procedure in this aspect with some differences. The major difference is that in their work they use the $Z - q_r$ relation, but in this paper the $R - q_r$ relation (R is the rainfall rate) is used. Detailed information will be given in the next section.

The Tropical Rainfall Measuring Mission (TRMM) is a joint mission between the U.S. and Japan, and it is the first satellite-based earth observation mission to monitor tropical rainfall. TRMM was launched by the H-II rocket from National Space Development Agency of Japan (NASDA)/Tanegashima Space Center in November 1997, and has moved into a circular orbit of altitude 350 km, inclination angle 35° and period 90 min. TRMM's precipitation radar (PR) is the first radar designed specifically for monitoring rainfall which will operate from space. The precipitation radar on the TRMM satellite enables us to clearly observe the three-dimensional storm structure over the ocean and land where no radar data of this kind has been available before. Since it was launched, much more progress has been achieved. In this paper, numerical simulations of two heavy rainfall cases that happened in 29–30 June and 1–2 July, 1998 in the Changjiang-Huaihe River basin, are performed with TRMM/PR radar data incorporated into the PSU/NCAR meso scale model MM5.

Although the TRMM satellite can cover the tropical and subtropical zone and can get the statistical precipitation of each month and year of the zone, it cannot give data for a continuous time for a given area. During a heavy rainfall, event, the satellite map only sample the event at one particular instant in its evolution. This is a problem when we incorporate TRMM/PR data into the numerical model at the initial integration time. But if we can get data from a radar network, we can incorporate the radar network data into the numerical model at the initial integration time instead of TRMM/PR data.

2. Method and data

2.1 *The model*

The nonhydrostatic version of PSU/NCAR mesoscale model version 5 (MM5) described in detail by Grell et al. (1993) is used. The model physics selected for this study is the Grell cumulus parameterization scheme. The model contains 145×126 grid points horizontally with grid intervals of $\triangle x = \triangle y = 40$ km, and the vertical integration domain is from the surface to 100 hPa with 23 layers of different heights. Two simulations are performed the control simulation (CTL) which uses surface and radiosonde data, and the sensitivity experiment (STE) in which TRMM/PR data are incorporated into the numerical model radiosonde and surface data.

2.2 *The method*

Many previous observational studies have shown that natural variations of the drop size distribution in time and space can lead to different $Z-R$ relations, ultimately producing different estimates of rain rates (e.g., Battan 1973; Ulbrich 1983; Austin1987; Huggel et al. 1996). The relation between Z and q_r (q_r is the mixing ratio of rainwater) is derived analytically by eliminating the rainfall rate between the expressions for the $Z-R$ and q_r-R relationships. From the definition of rainfall estimate R Eq.(1), moisture water content M Eq.(2) and reflectivity factor of the radar Z Eq.(3), we know the empirical Z–R and M–Z relations are of the form $Z = aR^b$ and $M = AR^B$ respectively. The relation between Z and M is $Z = A^{-b/B} a M^{b/B}$ and varies with the drop size distribution. Here a and b are not constant, yet if we assume the values of a and b are constant, then the value of M will deviate from the exact value. In the product of TRMM/PR 2A25, the parameters a and b are both functions of the rain type, existence of the bright-band, freezing height, storm height, and absolute height. Effects of the difference in the raindrop size distribution by rain type, the phase state, the temperature, and the difference in terminal velocity due to changes in air density with height are taken into account. The coefficient a is further modified by the index of non-uniformity. The rainfall estimates are calculated at different levels

from the attenuationcorrected Z-profile for the attenuation wave length by using a power law $Z=aR^b$. And the relation of q_r-M is $M=\rho q_r$. This indicates that the value of M varies with the drop size distribution. One hundred fifty-five Mei-yu rain drop spectra in the Nanjing area, sampled from 1980 to 1983, are analyzed and provide the value of A and B (Xu et al., 1987), $A=0.069$ and $B=0.89$.

Rainfall estimate:

$$R=\int_0^\infty \frac{1}{6}\pi D^3 N_D[\overline{V}(D)-W]dD \tag{1}$$

Moisture water content:

$$M=\int_0^\infty \frac{\pi}{6}D^3 N_D dD \tag{2}$$

Reflectivity factor:

$$Z=\int_0^\infty D^6 N_D f(\lambda, D)dD \tag{3}$$

Assuming $n_0=8\times10^6$ m^{-4}, yields

$$M=\rho q_r=0.069R^{0.89} \tag{4}$$

In the above, Z, M, q_r, and ρ are the reflectivity (units: mm^6 m^{-3}), moisture water content (g m^{-3}), mixing ratio of rainwater (g kg^{-1}), and the density of air (kg m^{-3}), respectively. Parameter D is the raindrop size (mm) and $N_D dD$ is the number of precipitation particles per unit volume per unit size interval. The parameter $\overline{V}(D)$ (m s^{-1}) is the terminal velocity of the rainfall and W (m s^{-1}) is the airflow ascending velocity. The function $f(\lambda, D)$ is the ratio of Mie backscatter area to Rayleigh backscatter area.

Table 1 gives the moisture water content in convective clouds (Flecher, 1962), yet some researchers have found that the moisture water content in convective clouds can reach 20–30 g m^{-3}. The order of the mixing ratio of observed vapor q_v in the layer of 850–700 hPa is about 10^{-1}–10^1 g kg^{-1}. So during convective rainfall the order of the mixing ratio of rainwater q_r is same as the order of the mixing ratio of vapor q_v, thus cannot neglect the mixing ratio of rainwater q_r during integration in the mesoscale model.

In this paper, numerical simulations of two heavy rainfall cases in the Changjiang-Huaihe River basin are carried out with TRMM precipitation radar data incorporated into the PSU/NCAR meso scale model MM5. The mixing ratio of rainwater q_r is obtained from the $R-q_r$ relation, and the mixing ratio of water vapor q_v in the model is replaced by $q'_v=q_v+q_r$. This procedure is used in order to consider both the mixing ratio of rainwater and that of water vapor in the model during integration. The Grell scheme is based on the rate of destabilization or quasi-equilibrium, and is a simple, single-cloud scheme with updraft and downdraft fluxes and compensating motion determining the heating/moistening profile. It is useful for smaller grid sizes 10–30 km, and tends to allow a balance between resolved scale rainfall and convective rainfall. This is a very simple scheme that was constructed to avoid first-order sources of errors. There is no direct mixing between cloud air and environmental air, except at the top and the bottom of the circulations. And no cloud water is assumed to exist; all water is converted to rain. From the moisture equation Eq.(5) and rainfall equation Eq.(8), the water phase state does not need to be known. And the moisture static energy equations Eq.(6) and (7) show that the addition of q_r will increase the moisture static energy and lead to the change of the heating and moisture profiles. The basic idea of the Grell scheme is very similar to that of the Arakawa-Schubert scheme, yet there are some differences between the two. The Arakawa-Schubert scheme considers the existence of multi-clouds, allows for entrainment into updrafts and allows for downdrafts, and allows liquid water to exist in the clouds. The basic physical meaning of the moisture equation (Grell scheme Eq.(5) below) is very close to Eq.(5.3.2.2.29) of the Arakawa-Schubert scheme (ref. Grell et al, 1993). But the right form of Eq.(5) does not contain terms which express the vertical change of suspended liquid water. If the parameter q in Eq.(5) is replaced by q'_v, (here $q'_v=q_v+q_r$, and q_v is the mixing ratio of vapor and q_r is the mixing ratio of rainwater), then Eq.(5) will have same meaning as Eq.(5.3.2.2.29) of Grell et al. (1993). So, the consideration of liquid water into the Grell scheme is feasible.

$$\left[\frac{\partial q(k)}{\partial t}\right]_{CU}=\frac{\partial q_u(z)m_b}{\partial z}-\frac{\partial \overline{q}(z)m_b}{\partial z}-\frac{\partial q_d(z)m_0}{\partial z}+\frac{\partial \overline{q}(z)m_0}{\partial z} \tag{5}$$

Table 1. Moisture water content in convective clouds (units: g m^{-3})

Moisture water content	Cumulus	Cumulus, cumulus congestus cloud	Cumulus congestus cloud, Cumulonimbus cloud
Average	0.18 – 0.64	0.6 – 1.0	0.4 – 1.0
Maximum	0.21 – 1.71	3.0 – 3.6	4.0 – 6.5

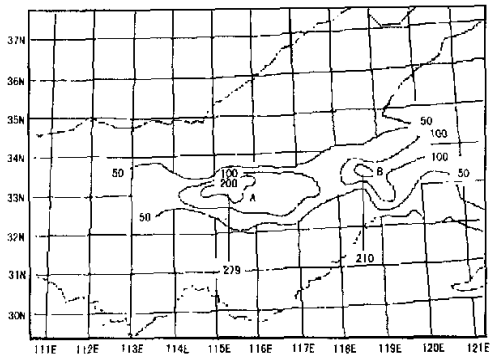

Fig. 1. Observed 24 hour accumulated rainfall from 0000UTC 29 0000UTC 30 June 1998 (units: mm).

$$\overline{h}(z) = c_p\overline{T}(z) + gz + L\overline{q}(z) \tag{6}$$

$$\left[\frac{\partial\overline{h}(k)}{\partial t}\right]_{CU} = \frac{\partial h_u(z)m_b}{\partial z} - \frac{\partial\overline{h}(z)m_b}{\partial z} - \frac{\partial h_d(z)m_0}{\partial z} + \frac{\partial\overline{h}(z)m_0}{\partial z} \tag{7}$$

$$R = I_1 m_b(1-\beta) \tag{8}$$

In the above, m_b is the mass flux of the updrafts at their originating level, m_0 is the mass flux of the downdrafts at their originating level, and $1-\beta$ is the precipitation efficiency. The overline denotes an environmental value, subscript u denotes an updraft property, and subscript d denotes a downdraft property. The term I_1 stands for the integrated condensate in the updraft. Here R stands for rainfall and h represents moisture static energy, q is the mixing ratio of vapor, g is the acceleration duetogravity, L is the latent heat, and c_p is specific heat at constant pressure.

2.3 *Data analysis*

The data used in this paper are the TRMM/PR rainfall estimates, 2A25. The domain of the data is the belt of Fig. 2 for the rainstorm of 29 June 1998, and of Fig. 6 for the rainstorm of 1 July 1998 respectively in the horizontal direction and 0–12 km in the vertical, with grid intervals of the data as $\triangle x = \triangle y = 5$ km and $\triangle z = 250$ m. Two procedures are used to treat the original data. In the horizontal direction, the maximum value around the model grid point is selected with a radius of 20 km. In the vertical, a partial Lagrange interpolation is used to insert the data into the model.

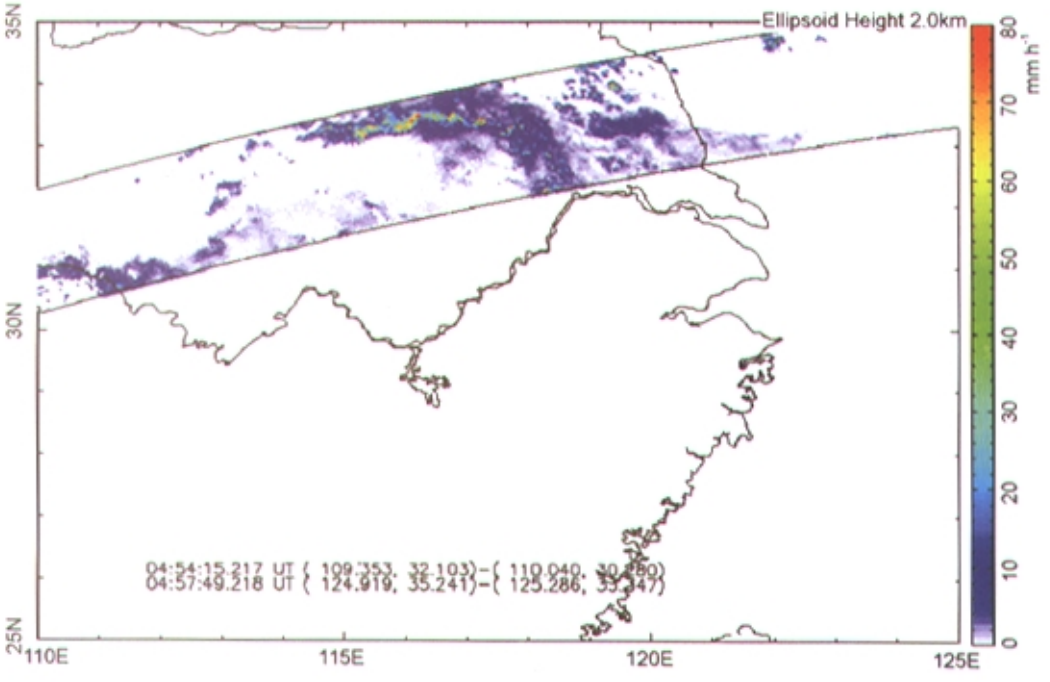

Fig. 2. TRMM/PR rainfall estimates at 2 km of height from 0454UTC to 0457UTC 29 June 1998, storm 1 (units: mm h^{-1}).

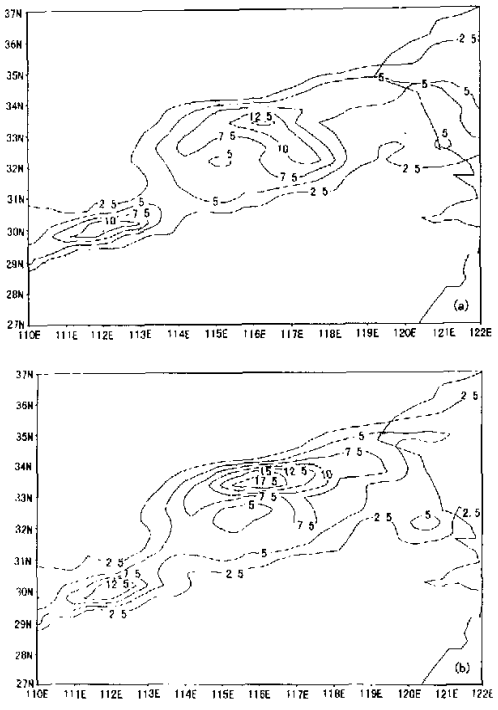

Fig. 3. Simulated 24 h precipitation of (a) CTL and (b) STE for 0000UTC 29 June to 0000UTC 30 June 1998, storm 1 (units: 10 mm).

3. Heavy rainfall cases and results

Turpeinen et al. (1990) indicated that three causes contribute to the spin-up problem: the initial specification of divergence, the initial moisture and thermal fields, and deficiencies in the physical parameterizations. The results in this section will show how the spin-up problem can be improved through the changing of the moisture field in the model.

3.1 *Rainstorm of 29 June 1998*

The severe rainstorm case of 29–30 June 1998 (storm 1) is used for numerical simulation. Figure 1 shows the observed 24 h precipitation for 0000UTC 29 to 0000UTC 30 June 1998, with 2 maximums of 279 mm and 214 mm located at A (115.5°E, 33.0°N) and B (118.5°E, 33.2°N) respectively. This severe rainfall event was formed mainly by a meso-α scale cyclonic vortex at 500 hPa situated in the upper reaches of the Huaihe River at 0000UTC to 0457UTC 29 June 1998, and this vortex moved eastward to the middle and lower reaches of the Huaihe River. The TRMM/PR data was incorporated into model at 0456UTC 29 June 1998. Figure 2 shows rainfall estimates from TRMM precipitation radar at 2 km of height from 0454UTC 29 June, 1998. There is a maximum rainfall belt located at (115°–117°E, 33° 34°N) at 2 km of height (Fig. 2), and maximum A is lacated in it. A another maximum rainfall is located at (110°–112°E). Results below show that both the heavy rainfall distribution and its maximum amounts in the sensitivity experiment (Fig. 3b) are improved over those in control experiment (Fig. 3a).

The simulated rainfall from CTL in the same time period as Fig. 1 is shown in Fig. 3a. The overall location of the rainbelt in Fig. 3a is roughly in accordance with that in Fig. 1, but the rainfall amount of maximum A (137.6 mm 24 h^{-1}) is much less than the observed amount, and maximum B is not even reproduced by the simulation.

The simulated rainfall amounts are improved in STE, as shown in Fig. 3b. In the figure, the value of maximum A is 180.9 mm which is obviously larger than in CTL, but maximum B is not reproduced either. The total rainfall is increased in STE. Furthermore, in CTL there is a fictitious maximum rainfall area (117°–118°E, 32°N) which does not exist in the observed field, yet in STE, this maximum rainfall area disappears. The moisture field located at A is increased in STE and the moisture field located at (117°E–118°E, 32°N) is changed little (the rainfall estimate is very small in this area). So, the incorporation of TRMM/PR is useful to improve the results of the numerical simulation of heavy rainfall. Figure 4 shows that in the moisture field, the maximum value of the rainbelt is increased greatly in STE, and there is a maximum area in Fig. 4b which is in the vicinity of A. Table 2 also shows that the spin-up problem can be improved through modifying the moisture field.

3.2 *Rainstorm of 1 July 1998*

On 1 July 1998, another rainstorm (storm 2) happened in the area from the south of the Huaihe River to Shandong Province. Figure 5 shows the observed total 24 h rainfall. In the figure, the rain-covered area is further north than that of Storn 1. There are four maximums and one is located at A (114.02°E, 33.36°N) with a value of 209 mm. The weather situation is similar to that of storm 1. At 500 hPa, a trough line lies from the Shandong Peninsula to Chongqing city. The trough line also, is located further north than that of storm 1.

The two storm cases happened in the Huaihe River basin and the weather situations of these two days are very similar, but there are still some differences. The maximum value of the storm 1 rainfall is larger than the

Table 2. Simulated precipitation maximum (mm) A of the control (CTL) and sensitivity experiment (STE) for four time intervals starting at 0000UTC 29 June 1998 (Storm 1)

Item	location	0–6 h	0–12 h	0–18 h	0–24 h
CTL	116.04E, 33.29N	45.2	99.7	129.4	137.6
STE	116.04E, 33.29N	51.8	132.2	172.9	180.9
observation	115.5E, 33.0N	169.0	245.0	257.0	279.0

Table 3. The location and temporal distribution of maximum A of CTL, STE and observation

Item	location	0–6 h	6–12 h	12–18 h	18–24 h	24 h total rainfall
Observation	114.02°E, 33.36°N	0.0	199.0	8.0	0.0	207.0
CTL	115.17°E, 34.39°N	0.0	58.2	81.5	39.3	179.0
STE	113.87°E, 33.27°N	22.2	95.3	35.6	6.3	159.4

storm 2 rainfall, and the area covered by the 200 mm isoline of the former is larger than that of the latter. The rain belt is oriented east-west in storm 1, but northeast southwest in storm 2. The time period of the strongest rainfall for storm 1 is in the first 12 h, but the strongest rainfall for storm 2 is in 6–12 h. Because of the spin-up problem, the result of the control experiment (Fig. 7a) evidently deviated from observation (Fig. 5). However, when the TRMM/PR data (Fig. 6) observed during 0406UTC to 0409UTC 1 July 1998 is incorporated into the model at 0408UTC 1 July 1998 (the sensitivity experiment, STE), the results (Fig. 7b) become close to observation.

It can be seen from Table 3, Fig. 5, and Fig. 7 that the location and temporal distribution of maximum A of STE is closer to observation than that of CTL. The temporal concentration of rainfall and the spin-up problem cause the position of A in CTL to be far from the observed. Because the moisture field is improved when a TRMM/PR data is incorporated into the model, the spin-up problem is improved, leading to better temporal and spatial distribution of the rainbelt. There are some unsatisfactory results in Table 3 however. The first is that the rainfall occurred earlier in STE, perhaps because the TRMM/PR data is incorporated into the numerical model two hours before the observed rainfall time. Another shortcomming of STE is that the maximum value is smaller than that of CTL. However, the total rainfall amount of the entire rainbelt in STE is larger than that of CTL, and maximum value of the three six-hour periods (from 6–24 h) is closer to observation than CTL, especial in the second six-hour period.

Thus, during the first few hours in CTL, the development of the simulated rainfall system does not do well, but develops strongly after the observed rainfall system disappears, hence the main cause of its deficiency. Walcott and Warner (1981) emphasized the importance of the adjustment of the humidity accompanying the diabatic initialization, and argued that if the environment is not humid enough, the upward motion associated with the initialized divergence field will not be sustained by latent heat release.

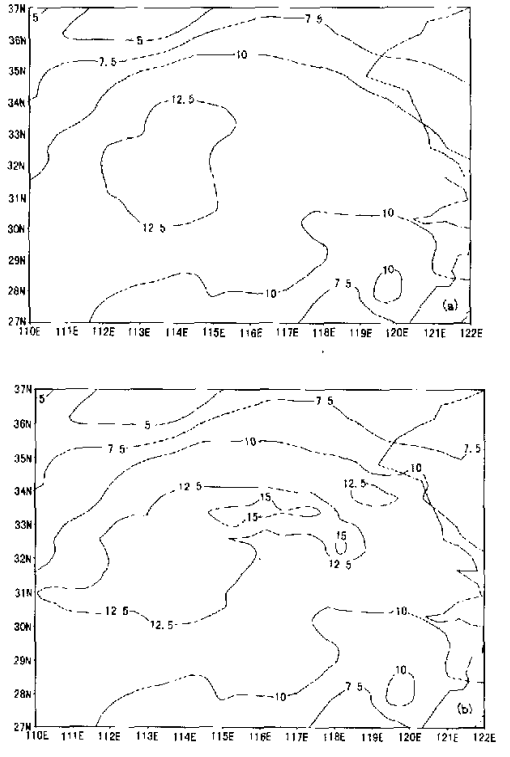

Fig. 4. Moisture field of (a) CTL and (b) STE at equal $\sigma = 0.7$ surface at 0456 UTC 29 June 1998, storm 1 (units: g kg^{-1}).

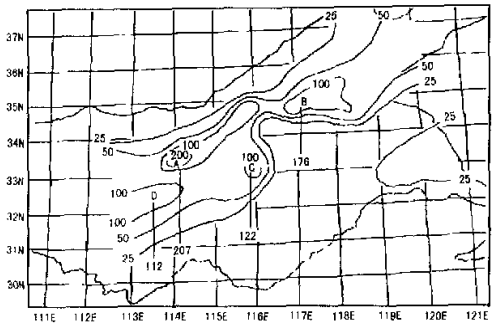

Fig. 5. Observed 24 hour accumulated rainfall from 0000UTC 1 July 0000UTC 2 July 1998 storm 2 (units: mm).

4. Conclusions

Two new modifications of a mesoscale model are introduced in this paper: (1) the improvement of the Grell scheme by consideration of liquid water, and (2) the incorporation of TRMM/PR data into the mesoscale model. According to the results of the above experiments, the following conclusions are given.

(1) The procedure of calculating q_r through the relation of R–q_r and incorporating TRMM/PR data into the mesoscale model using the relation $q'_v = q_v + q_r$ is feasible.

(2) The locations and maximum values of the heavy rainfall cases in the Huaihe River basin, via simulation with mesoscale model MM5 with incorporated TRMM/PR data, are evidently closer to the observations than those without TRMM/PR data.

(3) The spin-up time is shortened in simulations made using TRMM/PR data (STE) compared to experiments without using these data (CTL).

(4) The explicit influence of incorporating TRMM/PR data is the inclusion of mesoscale cloud clusters, which contain very large amounts of moisture content that would frequently be missed by only using conventional radiosonde data because the average distance between radiosonde stations is about 300 km.

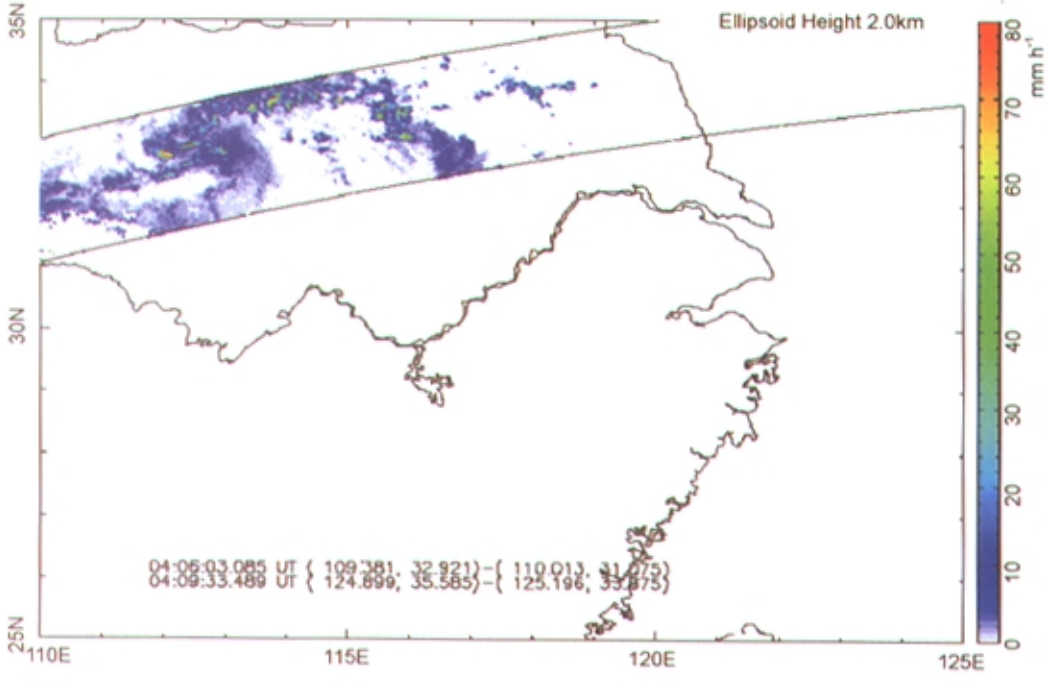

Fig. 6. TRMM/PR rainfall estimates at 2 km of height from 0406UTC to 0409UTC 1 July 1998, storm 2 (units: mm h^{-1}).

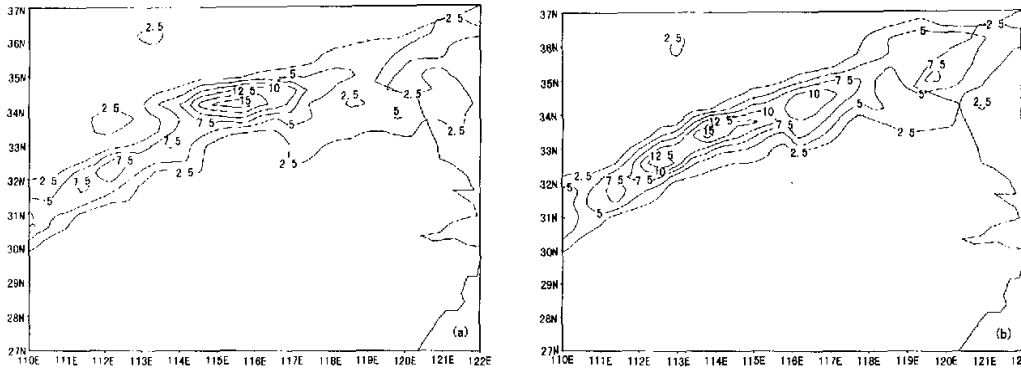

Fig. 7. Simlated 24 h precipitation of (a) CTL and (b) STE for 0000UTC 1 July 0000UTC 2 July 1998, storm 2 (units: 10 mm).

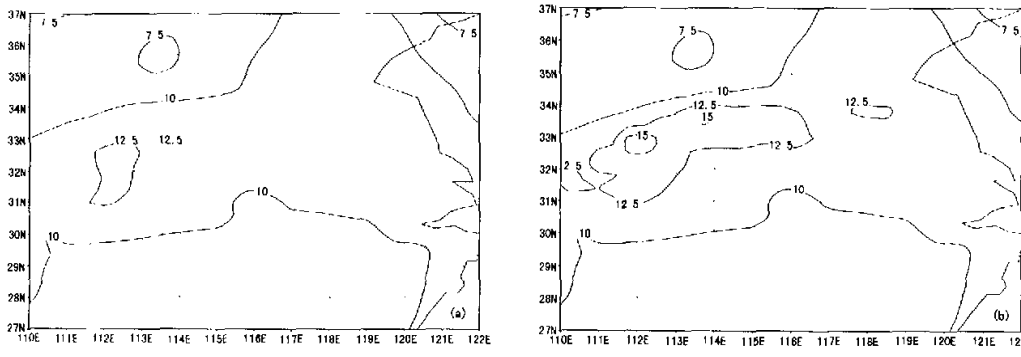

Fig. 8. Moisture field of (a) CTL and (b) STE at equal $\sigma = 0.7$ surface at 0408UTC 1 July 1998, storm 2 (units: g kg^{-1}).

(5) The spatial resolution of TRMM/PR data is very high, but the temporal resolution is very low. The satellitelsensor cannot capture the whole process of a heavy rainfall, which brings some deficiencies in the application of TRMM/PR data in the numerical model. When the growing radar network data becomes available for use in numerical models, it is expected that better results will be obtained.

Acknowledgments. This research was supported by the National Natural Science Foundation of China under Grant No.49794030.

REFERENCES

Austin, P. M., 1987: Relation between measured radar reflectivity and surface rainfall. *Mon. Wea. Rev.*, **115**, 1053–1070.

Battan, L. J., 1973: *Radar Observations of the Atmosphere*. University of Chicago Press, 324pp.

Ge Wenzhong, Dang Renqing, Jiang Dunchun, Xu Hui, and Takao Takeda, 1998: Application of radar and satellite data for numerical simulation of heavy rainfall. International Symposium on Mesoscale Water Cycle and Heavy Rainfall in East Asia. Nagoya, Japan, 2–4 Feb. 123–126.

Ge Wenzhong, Dang Renqing, Jiang Dunchun, Xu Hui and Takao Takeda, 1999: Application of radar and satellite data for real time numerical experiment and simulation of heavy rainfall. Workshop on Mesoscale System in Meiyu/Baiu Front and Hydrological Cycle. GAME/HUBEX Project Office. Xi'An, China, 3–9 Nov. 171–174.

Ge Wenzhong, Dang Renqing, Xu Zhifang, and Takao Takeda, 2000: The impact of assimilations of radar and satellite data on numerical simulation of heavy rainfall. International GAME/HUBEX Workshop, HoKKaido Univ., Sapporo, 93–96.

Grell A. G., J. Dudhia, and D. R. Stauffer, 1993: A description of the fifth generation PSU/NCAR Mesoscale Model (MM5). NCAR Tech. Note NCAR/TN-398 107pp.

Guo Xia., Dang Renqing, and Ge Wenzhong, 1999: The use of radar data in the numerical simulation of heavy rainfall in the Changjiang-Huaihe River basin. *Jour-*

nal of Tropical Meteorology, **15**(4), 356–362 (in Chinese).

Huggle, A., W. Schmid, and A. Waldvogel, 1996: Raindrop size distributions and the radar bright band. *J. Appl. Meteor.*, **35**, 1688–1701.

Jiang Dunchun, Dang Renqing, and Cheng Lianshou, 1994: The use of satellite data in the numerical prediction model for the study of the heavy rainfall caused by typhoon. *Journal of Tropical Meteorology*, **10**(4), 318 324 (in Chinese).

Kasahara, A. R. C. Balgovind, and B. B. Katz, 1988: Use of satellite imagery data for improvement in the analysis of divergent wind in the tropics. *Mon. Wea. Rev.*, **116**, 866–883.

Mills, G. A., and N. E. Davidson, 1987: Tropospheric moisture profile from digital IR satellite imagery: System description and analysis/forecast impact. *Aust. Meteor. Mag.*, **35**, 109–118.

Ninomiya, K., and K. Kurihara, 1987: Forecast experiment of a longlived mesoscale convective system in Baiu frontalzone. *J. Meteor. Soc. Japan*, **65**, 885–899.

Sun, Juanzhen, and N. A. Crook, 1997: Dynamical and microphysical retrieval from Doppler radar observations using a cloud model and its adjoint Part I: Model development and simulated data experiments. *J. Atmos. Sci.*, **54**, 1642–1661.

Turpeiner, O. M., L. Garand, R. Benoit, and M. Roch, 1990: Diabatic initialization of the Canadian Regional Finite Element (RFE) model using satellite data. *Mon. Wea. Rev.*, **118**, 1381–1407.

Ulbrich, C. W., 1983: Natural variations in the analytical form of the raindrop size distribution. *J. Climate. Appl. Meteor.*, **22**, 1764–1775.

Walcott, S. W., and T. T. Warner, 1981: A humidity initialization utilizing surface and satellite data. *Mon. Wea. Rev.*, **109**, 1989–1998.

Wang. W., and T. T. Warner, 1988: Use of four-dimensional data assimilation by Newtonian relaxation and latent-heat forcing to improve a mesoscale-model precipitation forecast: A case study. *Mon. Wea. Rev.*, **116**, 2593–2613.

Wang Pengfei, and Li Zihua, 1989: *Microcosmic Cloud Physics*. Lin Yuchen, Ed., China Meteorological Press, 163–164.

Xu Shaozu, Lei Lianke, Zhang Xueru, Gen Biao, and Xie Juyin, 1987: The characteristics of the microphysical structure of Mei-yu precipitation in the Nanjing area. *Journal of Nanjing University, Natural Sciences*, **23**(1), 175–185.

TRMM/PR资料在中尺度模式MM5中的应用

徐枝芳 葛文忠 党人庆 Toshio Iguchi Takao Takeda

摘 要

将中尺度非静力模式MM5中的积云参数化Grell方案作了改进，使它含有降水云的云水，即雨水含量，并用该模式对1998年6月29日08时-30日08时（北京时）和1998年7月1日08时–2日08时（北京时）发生在淮河流域的两次特大暴雨进行数值模拟研究，同时通过采用$R-q_r$关系将TRMM/PR（Tropical Rainfall Measuring Mission/Precipitation Radar）得到的降水强度资料R计算出比含水量q_r，然后用$q'_v=q_v+q_r$取代原模式中的比湿q_v。结果表明将TRMM/PR资料加入模式后，由于PR雷达具有较高的空间分辨率，能够很好地反映中小尺度系统的空间结构，能够使湿度值接近实际，缩短了中尺度系统的发展时间，使得模拟出来的降雨强度、雨量中心位置以及雨带形状更接近实况。

关键词：TRMM/PR, 数值模拟, 比含水量, 比湿, 暴雨, Spin-up问题, 积云参数化方案